SOME RECENT DEVELOPMENTS IN NUCLEAR CHARGED PARTICLE DETECTORS*

Herbert Stelzer

Gesellschaft fuer Schwerionenforschung
Darmstadt, W. Germany
and
Lawrence Berkeley Laboratory
Berkeley, California

Abstract: The latest developments of large-area, position sensitive gas-filled ionization chambers are described. Multi-wire-proportional chambers as position-sensing and parallel-plate-avalanche counters as time-sensing detectors at low pressure (5 Torr) have proven to be useful and reliable instruments in heavy ion physics. Gas (proportional) scintillation counters, used mainly for x-ray spectroscopy, have recently been applied as particle detectors. Finally, a brief description of a large plastic scintillator spectrometer, the Plastic Ball, is given and some of the first test and calibration data are shown.

1. Introduction

Nuclear particle detectors comprise such a wide range of elaborate and ingenious devices that it seems impossible to cover the progress made in this field during the recent years in one short talk. One has to make a selection and this selection is, of course, a matter of personal preference. After a few short remarks about a general classification of nuclear particle detectors, I will talk about gas-filled ionization chambers, low-pressure multi-wire-proportional chambers, parallel-plate-avalanche counters, gas scintillation detectors and finally, as an example of a detector with a non-gaseous medium, about a large plastic scintillator spectrometer. In each section I will describe one specific design in more detail to show the current state-of-the-art.

Nuclear radiation is detected via its interaction with matter and each detector can be characterized according to the type of interaction which is taken as the signature and the type of matter which is exposed to the radiation. Commonly used nuclear particle detectors can be roughly divided into those which look for the electrons liberated in a properly chosen medium and those which detect the light produced under the influence of the incoming nuclear radiation. I have tried to illustrate this classification scheme in Fig. 1.

The oldest of these detectors, beside the inorganic scintillator, is the gas-filled ion-chamber. The use of ion-chambers filled with liquid argon or xenon has spread widely since Willis and Radeka[1]) developed this type of detector for observing electro-magnetic showers in high-energy physics. Unfortunately, the severe recombination effects observed for heavily ionizing particles have made it impractical to use liquid ion chambers as nuclear particle detectors.

The second large group of "electronic" detectors includes all those, where, in the presence of a strong electric field, internal multiplication of the primary electrons occurs. The streamer chamber is still a widely used instrument, not only in high energy physics, but also in nuclear[2]) and heavy ion[3]) physics. The use of image intensifiers allows one to operate the streamer chamber at a lower E-field, which yields cleaner pictures and allows the use of less sensitive film with a higher dynamic range. This might be useful for possible particle identification via the streamer brightness. The currently available charged coupled devices open up the possibility to circumvent the use of film, which might facilitate and speed up data taking and data analysis.

Detection of e⁻-ion pairs
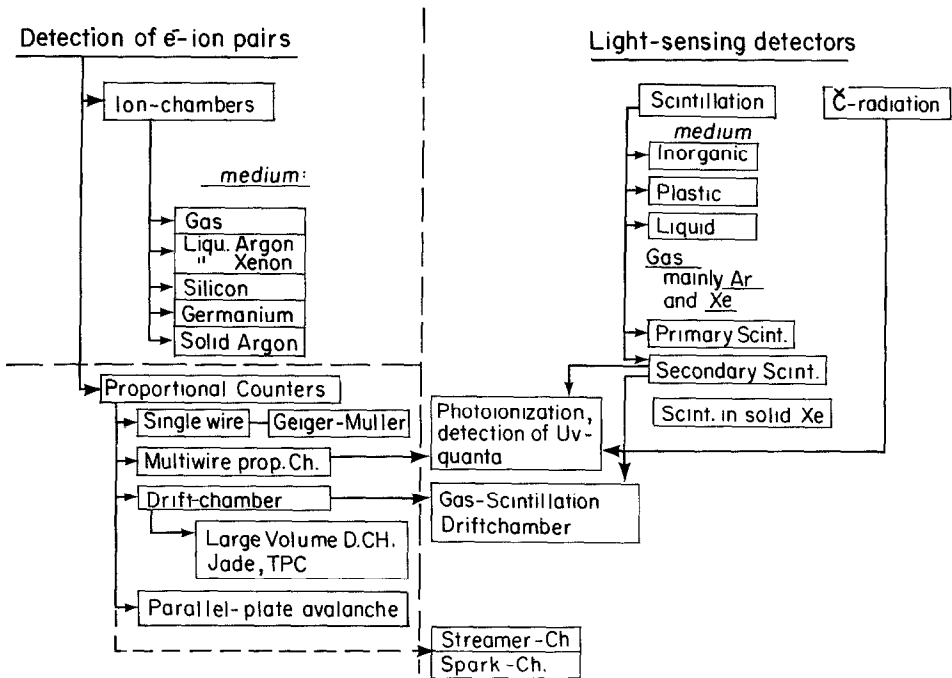
Light-sensing detectors

Fig. 1. Scheme of Nuclear Charged Particle Detectors.

The group of scintillation light sensing detectors can be divided into
inorganic, organic and noble gas scintillators. It is interesting to note that
in recent years new detectors have come into use, which form a link between the
light-sensing and electron-sensing detectors. In the gas scintillation drift
chamber[4]), for example, the time of arrival of the electrons at the anode is
measured via the scintillation light the electrons emit in the high E-field
around the wire. Such a crude classification scheme is of course not complete.
For example, the important group of nuclear track detectors[5]) and the secondary
electron emission detectors[6]) are missing.

2. Gas-Filled Ionization Chambers

The overwhelming success of gas-filled ionization chambers in the field of
nuclear particle identification is based on the fact that the number of liberated
electrons is, to a very high degree, a linear function of the energy lost in the
gas. This holds true for a wide range of projectile charges and projectile veloc-
ities. Only at very low energies, at some hundred keV, are non-ionizing collision
processes, like nuclear collision, important. The linear behavior of this detec-
tor depends on the fact that there is a fixed mean energy required to create one
electron-ion pair. This energy, usually called W, is around 25 eV for the commonly
used counting gases and about a factor of ten smaller for silicon detectors.
Numerous experiments have shown that W is practically independent, for a given
medium, of the type and energy of the incoming radiation.

The advantages of gas-filled ionization chambers, compared to solid state or scintillator counters, are linear behavior, no radiation damage, and easy adjustment to experimental requirements by simply changing the gas pressure. These last two features are of course especially important in the field of heavy ion physics. It is in this field where most of the recent developments of gas filled ion-chambers have occurred.

I will now discuss, as an example, a large area position-sensitive ionization chamber, which was recently built at GSI and already successfully used in several heavy-ion experiments[7]. The general lay-out of this chamber is based on an earlier design[8]. A serious problem often met in heavy ion experiments is the wide range of the energies and the nuclear charges of the reaction products to be identified in the ion-chambers. Let me illustrate this with the reaction 8 MeV/amu U on Ca. The projectile-like nuclei have an energy between 2 and 5 MeV/amu and the target-like nuclei lie between 0.5 and 12 MeV/amu. Table 1 shows the ranges of these particles in 250 Torr methane. The depth of the chamber must consequently be about 100 cm. Of course, a higher gas-pressure would reduce the ranges, but there are two reasons against it: 1) low energy particles would stop directly behind the entrance window and always slight inhomogeneities of the electric field are present there, 2) a higher gas pressure implies a thicker entrance window which causes more energy- and angle-straggling.

Table 1. Ranges of ^{40}Ca and ^{238}U.

	Energy (MeV/amu)	Range (cm) in 250 Torr CH_4
^{40}Ca	0.5	3.4
^{40}Ca	12.0	90
^{238}U	2.0	16
^{238}U	5.0	33

The Z-identification is done by the usual ΔE-E_{Rest} measurement. An optimum Z-resolution is obtained when the ratio of ΔE:E_{Rest} is about 1. The large dynamic range in the nuclear charge of 1:5 requires a subdivision of the anode in several independent electrodes, which makes it possible to form an optimum ΔE:E_{Rest} ratio over the whole energy- and Z-range. These considerations led to the design as shown in Fig. 2. The chamber is built as a twin ionization chamber with one common cathode (the separate cathode plates shown in the figure are coupled electrically together). The chamber is designed for the acceptance of all the particles which hit the entrance window and come from a point-source (the target), located 1 m in front of the entrance window. The window (2μ Hostaphan) is 2 x 60 mm high and 400 mm wide. The anode plates dE_1, dE_2, dE_3 and E_{Rest} are 60, 60, 200, and 840 mm long in the direction of the particle track. The active depth of the chamber is thus 1160 mm. The distance between cathode and Frisch-grid, which runs parallel to the anode, is 90 mm at the chamber entrance and 180 mm at the end. The distance between Frisch-grid and anode is 30 mm. The θ-grid between Frisch-grid and anode is made of 50μ wires which run parallel to the particle trajectory. The wire-spacing is 1 mm at the chamber entrance and 2.5 mm at the chamber end. This grid measures the in-plane scattering angle. When the primary electrons drift to the anode, they induce a signal on the nearest wire when they pass through the θ-grid. The wire is read out via a L-C-delay line method. Since the diffusion of the electrons on their way to the anode (<0.1 mm per cm drift-path) is small, a position resolution of about 2 mm is achieved. The out-of-plane angle is measured via the time-difference between the cathode and the anode-signal. The cathode-signal is prompt with the particle, but the signal on the anode appears only when the electrons have passed the Frisch-grid. The time-difference is thus
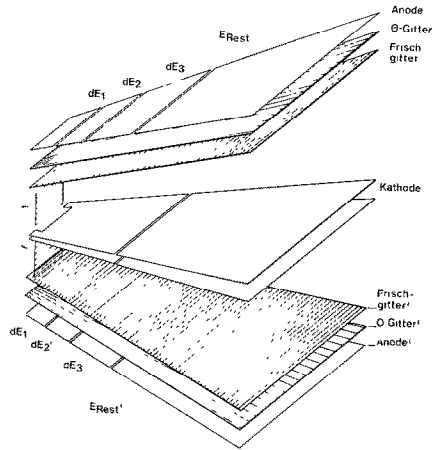
Fig. 2. The big position-sensitive ionization chamber at GSI. The active volume
is 120 x 400 x 1200 mm.

proportional to the distance between the particle trajectory and the Frisch-grid.
A resolution of $\leqslant 1$ mm is obtained.
    The voltage applied to the cathode with respect to the grounded Frisch-grid
is chosen in such a way as to maximize the drift velocity of the electrons in
the active volume of the chamber. The relative field strength on both sides of
the grids and the geometry of the grids themselves are such that the number of
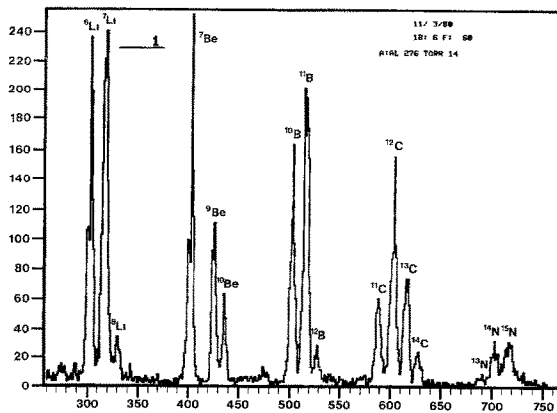electrons lost on them is negligible.

Fig. 3. Separation of isotopes with ΔE-E measurement in the big ion chamber.

The signals from the four anode plates are conveyed to the computer through standard electronics consisting of charge sensitive preamplifiers, main amplifiers and analog-to-digital converters (CAMAC-modules). The ΔE-signal is obtained by summing the signals from the first plate(s), depending on the range of the particle, such that the total ΔE-signal is about equal to the rest-energy E_{Rest}. Fig. 3 shows a Z, M distribution derived from a ΔE-E measurement in this chamber[9]. The experiment was done with a 86 MeV/amu ^{12}C-beam on an Al-target. The isotopes up to nitrogen are clearly separated. In another experiment with 8 MeV/amu ^{238}U on ^{48}Ca the projectile-like fragments were identified with a Z-resolution of $Z/\Delta Z = 92$[7]. This demonstrates that this big ionization chamber is as well suited for light and for heavy ions. The resolution of the total energy is $\leqslant 1\%$.

3. Multiwire Proportional Chambers at Low Pressure

Multiwire proportional chambers (MWPC) have grown, since their invention by Charpak in 1968, into the most widely used and most versatile detection system in high energy physics. It is an obvious idea to try to adapt this elegant detection scheme for heavily ionizing particles[10]. These particles have a mugh higher ionization density and subsequently, the chamber can be operated at a pressure much lower than atmospheric pressure. This low pressure facilitates the operation of such a detector in a vacuum-chamber, since now the entrance window can be made thin in order to reduce energy loss and straggling of the incoming particles.

Let me now briefly describe how we have built a MWPC for heavy ions[11]. Fig. 4 shows a perspective view of the counter. The anode wires are spanned in a diagonal direction, the cathode planes are mounted at 15 mm distance on both sides of the anode plane. Two read-out planes with the wire direction orthogonal to one another, are placed at 5 mm distance from the anode plane. All the wire planes consist of 50 µm copper-beryllium wires with a spacing of 2 mm. The negative signal on an anode wire nearest to the track of the heavy ion will induce a positive charge on both read-out planes A_1 and A_2 and the determination of the charge carrying wires will yield the x and y positions with only one multiplication wire plane. The sensitive area of the chamber is 88 x 88 cm^2 and is operated at 10 Torr i-butylene or less.

The read-out is done by means of the current-division method. All the wires of A_1 (resp. A_2) are soldered to a 88 cm long discrete resistor-chain[12]. The resistance between adjacent wires is 100 Ω. Every 80 mm along the chain the signal is taken off and fed into current sensitive amplifiers the output of which is directly applied to charge sensitive ADCs. The signals are fast and can be gated by a 300 ns logic signal. Consequently the counter can sustain high counting rates ($>10^5$ counts/s). The position resolution achieved is 2 mm FWHM.

Cathode   - 800 V
Read-out A1   0 V
Anode   +700 V
Read-out A2   0 V
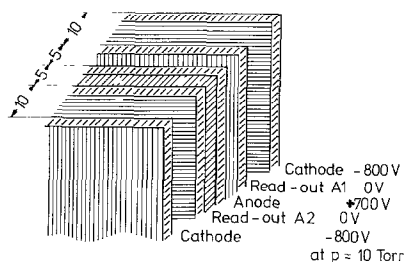Cathode   - 800 V
at p = 10 Torr

Fig. 4. Perspective view of a multiwire proportional counter with two additional readout planes. The potentials applied to the different planes at a gas pressure of 10 Torr are also indicated.

With other similar interpolating read-out systems a resolution much better
than the wire-spacing is obtained. The relatively poor resolution in this case
can be explained by events where the primary electrons are spread, either due
to transversal diffusion or to photon propagation, causing two adjacent wires
to develop an avalanche[13].
    A very astonishing result has recently been reported by Breskin et al.[14].
They operated their 4 x 4 cm^2 MWPC, equipped with 10μ anode wires, at a pressure
below one Torr and observed with oxygen ions a time-resolution of 100 ps FWHM.
In a counter with wires as the signal-sensing elements one should not expect a
time-resolution much below 1 ns due to the non-uniform electron drift paths.

4. Parallel-plate Avalanche Counter (PPAC)

This detector was introduced by Christiansen nearly 30 years ago, but it
was seldom used until its introduction in heavy ion physics several years ago[15].
Today this counter can often be found as timing detector for heavily ionizing
radiation. A PPAC consists simply of two thin metalized foils mounted parallel
with a small gap of 1 or 2 mm in between. The counter is operated at several mb
hydro-carbon gas, like i-butane, and a strong electric field E can be maintained
in the gap. Due to this high reduced field, E/p, (p is the gas pressure) a gas
multiplication factor around 5000 is achieved. On the anode a very fast negative
signal of several mV pulse-height is observed. The rise-time ranges from 1 ns
for a small counter to 5 ns for a 900 cm^2 counter. This fast-rising signal can,
at least qualitatively, easily be understood by the following considerations.
The growth of the electron avalanche is determined by an exponential law N $\sim$
exp($\alpha \cdot$d) where α is the first Townsend coefficient and d is the drift path.
From this it is clear that the primary electrons starting near the cathode
contribute most to the signal (Fig. 5). The mean free path for ionization is
given by 1/α and during the drift-time of the avalanche across this distance
the anode signal builds up. Assuming α = 100 cm^{-1} and a drift-velocity of
10 cm/μ sec (which are not unreasonable considering the high E/p value of
500 V/cm. Torr), one gets a signal rise-time of 1 ns, the value which is also
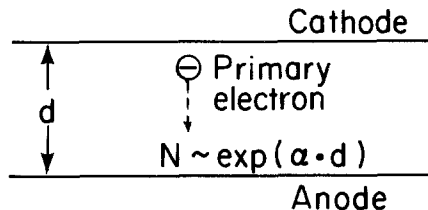observed experimentally.

Fig. 5. Gas multiplication in a PPAC.

The attainable time-resolution depends, of course, on the size of the
avalanche counter. With 1 cm^2 counters we have measured a time-resolution of
120 ps (FWHM) against the high-frequency of the well-tuned UNILAC accelerator.
With larger counters, 200 ps (FWHM) under experimental conditions are attainable.
The timing of the output signal of a PPAC depends on the impact point of the
particle on the counter surface. For small counters this effect is negligible,
but for 30 x 30 cm^2 detectors this shift in the timing may reach 2 ns and this
x-y dependence must be carefully calibrated. Three contributions to this effect
can be distinguished: 1) the finite velocity of the timing signal from the impact
point to the amplifying circuit, (this signal velocity has been measured to be
2/3 of the velocity of light), 2) geometrical imperfections in the parallelism
of the two electrodes, and 3) the attractive electrostatic forces between the
two foils, which tend to decrease the gap in the middle of the counter.

PPAC's can easily be made position sensitive by inserting a grid of wires between anode and cathode. The second coordinate is obtained by subdividing the cathode into stripes, which run orthogonal to the wires (Fig. 6a). The induced charges on the stripes and the wires can be read out directly or via an inter-polating read-out method such as the delay-line or charge division method. As long as the separation between the cathode-stripes is small (~0.3 mm) and the potential on the wires is such that the electric field remains homogeneous, the timing property of the counter is not degraded.
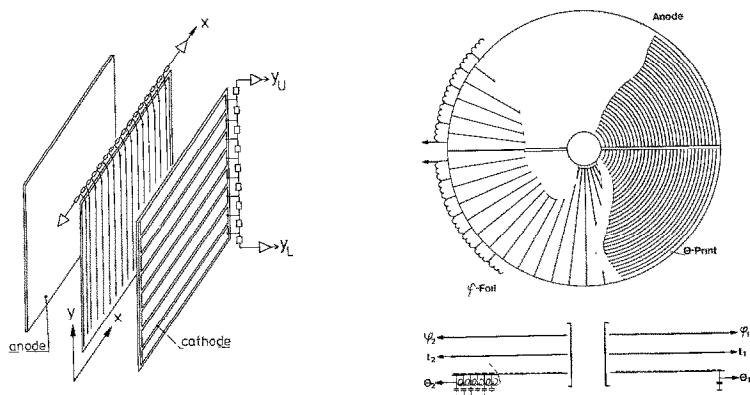

Fig. 6. Position-sensitive avalanche-counters.
         (a) read-out of the induced charges on a wire-grid and on cathode
              stripes. (b) determination of the angles θ and φ.

As an example for the flexibility one has in the design of this type of detector I will briefly describe a counter designed to identify binary fission reactions (Fig. 6b)[9]. The circular counter with a diameter of 30 cm is placed 40 cm downstream of the target, the beam passes through the hole in the middle of the counter. The detector has three electrodes, all of them are split electri-cally into two half-circles. The outer electrodes are cathodes, the medium electrode is the anode, a 2μ Hostaphan-foil uniformly evaporated with a thin gold-layer on both sides. From this foil the timing-signals t_1 and t_2 for the upper and the lower half are derived. The first cathode, the φ-foil, provides the φ-angle of the reaction products and is evaporated with a pattern of radial stripes with an angular spacing of 6°. These stripes of each half-circle are connected to a delay-line (1.5 ns per stripe). The background cathode, the θ-print, consists of concentric half-circles on a printed circuit board. The rings have an angular spacing of 0.7° and they are connected on the backside of the board to a delay-line. This electrode determines the scattering angle . The two fragments from a binary fission process will always hit, for kinematical reasons, both half-circles of the counter and the measurement of θ, φ, and the time-difference between them completely determines the kinematic. A draw-back of this counter is the pronounced position dependence of the timing output.

The total thickness of a start-detector in a TOF-system is of major importance. In a recent experiment at the Bevalac we used position-sensitive avalanche counters as start detectors and silicon-surface-barrier detectors for the stop signal[16]. The avalanche counters, with a sensitive area of 50 cm² were constructed with silver coated Formvar foil electrodes and stretched Polypropylene windows to contain the gas. The total thickness of such a counter was 150 μg/cm², as determined by an energy-loss measurement. The TOF-telescope was frequently

calibration with α's and fission-fragments from a [252]Cf-source. The timing-peaks of the α's and the fragments allow a measurement of the plasma-delay of this TOF-system. We measured a plasma-delay of 1.5 ns, which is very close to the published value of 1.8 ns for silicon-surface-barrier detectors[17]). This shows that, if at all, there is only a weak dependence of the timing output of an avalanche counter on the type of the incoming particle.

In an avalanche counter, operated at about 5 to 10 mb gas-pressure, one needs about 500 primary electrons to obtain a decent timing signal with good signal-to-noise ratio. This is about the amount of primary ionization produced by a 5.5 MeV α-particle. If one has to deal with less ionizing particles, one has to find some way to increase the primary ionization. A higher gas pressure will deteriorate the signal rise-time, but on the other hand the signal-to-noise ratio will improve. A group[18]) at LBL is currently working on a PPAC for minimum ionizing particles, operating at atmospheric pressure. They use neon with a small admixture of acetone as the counting gas. A signal rise-time of about 8 ns is observed and the signal-to-noise ratio is good enough so that a time-resolution in the 100 ps range appears to be possible.

5. Gas Scintillation Counters

Gas scintillation counters detect the light emitted by a gaseous medium which is exposed to nuclear radiation. Noble gases are the most efficient scintillators and they are the only one which are widely used. The gas pressure in these detectors vary over a wide range between 100 Torr and several thousand Torr. Recently, A. J. Policarpo has reviewed very exhaustively gas scintillation counters and in the following I will often make use of this excellent review article[19]).

Basically two types of scintillation light can be distinguished; simply, the primary light and the secondary light. The primary light originates from the radiative de-excitement of the medium which was excited by the incoming nuclear radiation. It is fast, with a rise-time of <20 ns and a decay time between a few ns and some hundred ns. The light output is a linear function of the energy deposited by the incoming nuclear radiation which compares favorably with the saturation effects in plastic scintillators. Another light emission process occurs, the so-called secondary or proportional scintillation, when an electric field is applied to the interaction region. The primary electrons gain enough energy to undergo inelastic but non-ionizing collisions. Recently Suzuki and Kubota[20]) measured the emission spectra of the proportional scintillation of noble gases and clarified the mechanisms of the light emission process. The secondary light emission is attributed to the radiative de-excitation of excited molecular states of the noble gas and the emission spectra are continua in the ultraviolet region with narrow peaks which are characteristic for each noble gas. The peak positions for argon, krypton and xenon are 1280 Å, 1470 Å and 1730 Å. Cumpstey and Vass[21]) developed a model which describes the formation of the secondary scintillation, assuming that the dominant excitation process in the gas occurs by electron impact, which seems to be the case at a reduced field strength (= field strength divided by the gas pressure) above 2 V/cm·Torr[22]). When the electric field strength is raised above the value where charge multiplication sets in (the proportional counter region), the then formed secondary electrons also participate in the light emission process.

The light yield is, within certain limits of the field strength, an approximately linear function of the reduced field strength. The light gain of the secondary scintillation, relative to the primary light, is of the order of several hundred. The attainable energy resolution is basically determined by the ratio of light output to deposited energy. It turns out that this ratio is about 100 times larger than that of a NaI(Tl) crystal. The decay time of the secondary light is, of course, related to the drift time of the electrons to the anode. The decay time of the excited molecular states ranges from 3200 ns for argon to 90 ns for xenon[23]).

A crucial factor in the reliable and stable operation of a gas scintillation counter is gas purity. Impurities have to be kept in the ppm range, otherwise severe quenching of the light output occurs.

One drawback of the gas proportional scintillation counter is that the emitted light lies in the ultraviolet region. Photomultipliers with quartz windows and wave-length shifters, like p-terphenyl, have to be used. In a practical design of such a counter the problem of achieving uniform light collection efficiency has to be born in mind.

To conclude these general remarks about gas scintillation, one may state that large area gas proportional scintillation counters are now a well developed detector, mainly used in the field of x-ray spectroscopy. Much of this detector development has been done by Policarpo and his collaborators. Typically a gas proportional scintillation counter gives <10% resolution for 5.9 keV γ's, about a factor of two better than ordinary gas proportional counters. Xenon seems to be best suited as the filling gas. It has a high stopping power, produces more electron-ion pairs per energy spent in the gas, the emitted light pulses show a faster rise- and decay-time and the emitted uv-photons lie in the range of 1500-1950 Å, which means they can be detected by means of a photomultiplier with quartz-windows, without the use of wave-length shifters.

In the recent years a group at Darmstadt has devoted much work to the development of a gas scintillation counter for heavy ions. These heavily ionizing particles produce so much primary scintillation light that no further light amplification via secondary scintillation in an electric field is necessary.
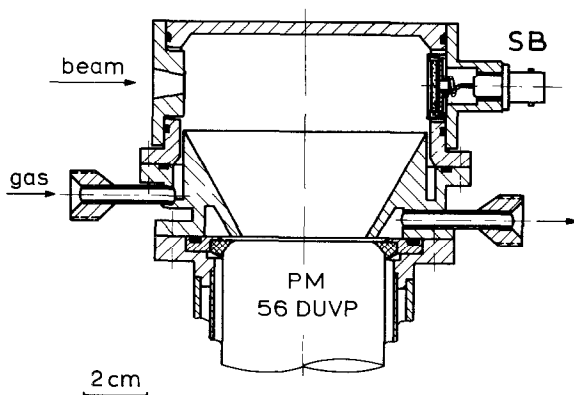

Fig. 7. Gas-scintillation counter (GSC) with built-in surface-barrier detector (SB).

Fig. 7 shows the basic design of their detector[24,25]. The gas-volume is viewed by a photomultiplier with a quartz-window. The inner chamber walls are coated with MgO as a reflector and a wavelength shifter (p-terphenyl). The gas scintilation counter serves as an energy-loss detector, the residual energy of the heavy ion is measured in the surface barrier detector SB. The counter is typically operated with pure argon or pure xenon at some hundred Torr. An energy resolution of 1.6% was achieved when 290 MeV Pb ions were stopped in the gas. This resolution is about two times worse than what is typically achieved with a gas ionization chamber of comparable size. As already mentioned, a pulse-height defect or quenching does not exist in gas scintillators, but conversely, a pulse-height excess (compared to α-particles) is observed[26]. This increase in light-output for very heavily ionizing particles like 1.4 MeV/amu Pb can be explained by recombination luminescence. This pulse-height excess amounts to several percent. It can be switched off by applying a small electric field to the interaction volume to separate more quickly the charge carriers which is anyway necessary to increase the high-count rate capability.

Since only the fast primary scintillation light is used in this gas scintillation counter, it is well suited for timing measurements. A time resolution of 210 ps has been achieved with this counter, and in this respect, a gas scintillation counter is superior to an ionization chamber.

To overcome the difficulties connected with photomultipliers, like bulkiness and peak-shifts at high count rates, and the wave-length shifter, which shows a poor quantum efficiency and tend to degrade the required purity of the scintillating gas, several groups are working on alternative light-sensing detectors. Van Staden et al.[27] replaced the photomultiplier of their gas scintillation counter by a cooled vacuum photodiode and achieved satisfactory results, at least for very heavy ions. Another very promising approach is the coupling of
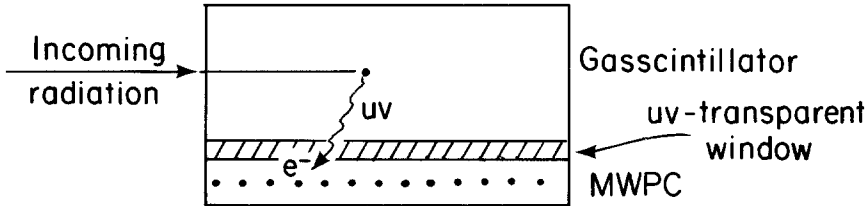

Fig. 8. Principle of a photoionization detector

a gas scintillation counter to a photoionization detector[28,29]. The principle of operation is the following (Fig. 8). A gas scintillator or a gas proportional scintillator is separated from a multi-wire-proportional chamber (MWPC) by a ultraviolet-transparent window (like lithiumfluoride). The MWPC is filled with the usual gas-mixture plus an admixture of some percent of an organic vapor with a low enough photoionization threshold. The uv-quanta of the scintillation process enter the MWPC and there an efficient photoionization process on the molecules of the admixture takes place. The single photo-electrons develop into an avalanche and are detected and localized in the usual way. One problem with this detection scheme is to find a uv transparent window and an organic vapor with a sufficiently low photoionization threshold, a problem which has been for Xe not yet solved.

Much work has been done to apply this method of imaging ultra-violet radiation in Cerenkov-detectors[30,31]. This approach seems to be especially suited to image the Cerenkov-light produced by relativistic heavy ions, since the photon yield is much higher (the light-yield depends on Z^2, Z being the charge of the radiating particle)[32].

6. Plastic Scintillator

Nearly every substance, when hit by ionizing radiation, scintillates and emits light in the visible or ultraviolet region, and scintillation materials nowadays in use are distinguished by their unusually high efficiency in light output. Modern plastic scintillators consist of a bulk material, composed mainly of benzene rings and doped with a small amount of impurity. Sometimes a wave-length shifter is added to match the emitted light better to the photomultiplier response. For a detailed discussion of the physical aspects of the scintillation process I refer to the textbook of J. Birks[33].

It is a well known fact that the light-output of a plastic scintillator is linear in the deposited energy only for electrons above 100 keV, but saturation effects occur for non-minimum ionizing particles. This distinct behavior, compared to a gas-filled ion chamber, has recently been pointed out again by Ahlen[34]. The luminescence per unit pathlength of the particle in the scintillator, dL/dx, approaches a constant value at large dE/dx values. The light output can be expressed as a function of the range of the heavily ionizing particle in the scintillator, at least for energies up to 15 MeV per nucleon[35]. For

relativistic heavy ions the scintillator response becomes again unsaturated[36]), e.g., the light-output is proportional to the energy spent in the scintillator. This behavior can, at least, qualitatively, be explained in a model proposed by Meyer and Murray[37]) and by R. Voltz et al.[38]). The scintillation light arises from two sources: 1) a primary column of ionization centered around the path of the ion and 2) δ-rays which escape from the primary column. These δ-rays produce light with high efficiency, whereas in the ionization column quenching occurs, which results in saturation effects. It is the relative importance of these two sources which determines the response of a scintillator to ionizing radiation. A relativistic heavy particle like neon at 400 MeV/amu produces a lot of high energy δ-rays and the linear response of the scintillator is at least partly restored. For relativistic light ions the response of the scintillator remains non-linear with the deposited energy[39]). The response of scintillators to relativistic heavy ions is treated in more detail in another contribution to this conference[32]).

I will now briefly describe the Plastic Ball[40]), which is currently being built for experiments at the Bevalac. The plastic scintillator detector, which covers a solid angle of nearly 4π, is capable of recording very high-multiplicity events, as are often observed in relativistic heavy-ion collisions. It can measure the energy-loss and total energy of each detected particle and thus allows charged particle identification up to ^{4}He. For experiments at the upcoming heavy-ion accelerator Saturn a 4π-detector with similar goals, but of completely different design, is under construction[41]).
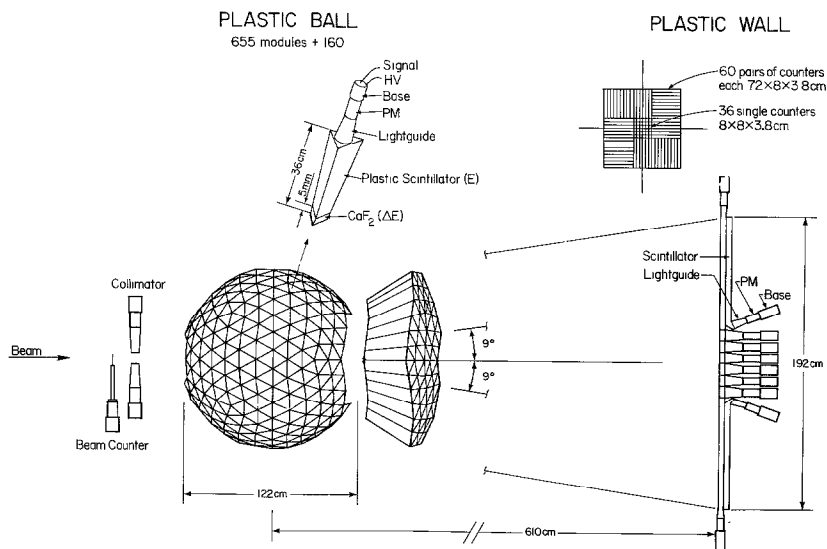

Fig. 9. Schematic drawing of the 4π spectrometer, with sketch of one of the CaF_2-plastic scintillator modules.

Fig. 9 shows a schematic drawing of the plastic scintillator spectrometer. The geometry has been adopted, with minor modifications, from the Stanford crystal ball detector for γ-rays. The total number of modules is 815. Each individual detector module is a "phoswich", consisting of a 4 mm thick CaF_2 scintillator glued to a 350 mm long plastic scintillator NE 114. It has the shape of a truncated pyramid and is viewed, via a conically shaped lucite light-guide, by one photomultiplier. The calcium fluoride scintillator measures the ΔE and the plastic scintillator measures the residual energy of the particle. The extremely different decay times of the CaF_2 and the plastic (1 μs and 5 ns resp.) allows the separation of their light output by integrating the PM-signal during the first 20 ns (the "fast" energy-signal) and then integrating the signal for 2μ sec, which yields the ΔE signal. In this way a simple, low cost and efficient ΔE-E measurement with one photomultiplier per module is achieved. This ΔE-E telescope provides particle identification ranging from protons with 30 to 210 MeV energy up to ^{4}He with 135 to 980 MeV. Positive pions with an energy of 15 to 120 MeV can be identified as well with an additional electronic scheme which looks for the delayed coincidence from the π-μ-decay.
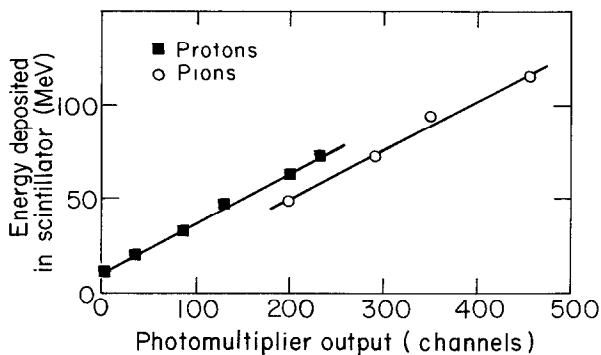

Fig. 10. Energy-calibration on one Plastic ball module with protons and pions.

Due to the above discussed saturation effects in the scintillator light output and due to a light collection efficiency which depends on the particle range, a careful calibration of each module has to be performed. This work is currently under way and Fig. 10 shows the energy deposited by protons and pions in one module plotted versus the photomultiplier output. For each particle the PM-output is approximately linear with the deposited energy (the lines are drawn by eye), but there is a clear shift between the protons and the weaker ionizing pions.

References

1) W. J. Willis and V. Radeka, Nucl. Instr. and Methods, 120 (1974) 221.

2) K. van Biber et al., contribution to this conference.

3) J. P. Brannigan et al., contribution to this conference.

4) K. P. Schelhaas, M. Mutterer, J. P. Theobald, P. A. Schillack, G. Schrieder and P. Wastyn, Nucl. Instr. and Methods 154 (1978) 245 and references there.

5) Proc. of the Int. Spring School on the Development and Applications
    of Solid State Nuclear Track Detectors, Nucl. Instr. and Methods 173
    (1980) No. 1.

6) P. Wastyn, M. Mutterer and J. P. Theobald, GSI Annual Report 1978,
    p. 180.

7) G. Augustinski, H. Sann, and A. Olmi, GSI Annual Report 1979.

8) H. Sann, H. Damjantschitsch, D. Hebbard, J. Junge, D. Pelte, B. Povh,
    D. Schwalm and D. B. Tran Thoai, Nucl. Instr. and Methods 124 (1975)
    509.

9) A. Gobbi, U. Lynen et al., private communication.

10) F. Binon, V. V. Bobyr, P. Duteil, M. Gouanere, L. Hugon, M. Spighel
    and J. P. Stroot, Nucl. Instr. and Methods 94 (1971) 27.

11) U. Lynen, H. Stelzer, A. Gobbi, H. Sann and A. Olmi, Nucl. Instr. and
    Methods 162 (1979) 657.

12) R. Chaminade, J. M. Durand, J. C. Faivre and J. Pain, Nucl. Instr. and
    Methods 118 (1974) 477.

13) J. Stähler, G. Hemmer and G. Presser, Nucl. Instr. and Methods 164 (1979)
    305.

14) A. Breskin, R. Chechik and N. Zwang, Nucl. Instr. and Methods 165 (1979)
    125.

15) H. Stelzer, Nucl. Instr. and Methods 133 (1976) 409.

16) H. Stelzer and A. Baden, Nuclear Science Annual Report 1979/80, Lawrence
    Berkeley Laboratory, Berkeley.

17) H. Henschel and R. Schmidt, Nucl. Instr. and Methods 151 (1978) 529.

18) V. Perez-Mendez, private communication.

19) A. J. P. L. Policarpo, Space Sci. Instr. 3 (1977) 77.

20) M. Suzuki and S. Kubota, Nucl. Instr. and Methods 164 (1979) 197.

21) D. E. Cumpstey and V. G. Vass, Nucl. Instr. and Methods 171 (1980) 473.

22) Yu. A. Butikov, B. A. Dolgoshein, V. N. Lebedenko, A. M. Rogozhin and
    B. U. Rodionov, Sov. Phys.-JETP 30 (1970) 24.

23) R. Brodmann and G. Zimmerer, J. Phys. B10 (1977) 3395.

24) M. Mutterer, J. P. Theobald and K. P. Schelhaas, Nucl. Instr. and
    Methods 144 (1977) 159.

25) M. Mutterer, J. Pannicke, K. P. Schelhaas, J. P. Theobald and
    J. C. van Staden, IEEE NS 26, No. 1 (1979) 382.

26) M. Mutterer, J. Pannicke, K. Scheele, W. Spreng, J. P. Theobald and
    P. Wastyn, IEEE NS 27, No. 1 (1980) 184.

27) J. C. van Staden, J. Foh, M. Mutterer, J. Pannicke, K. P. Schelhaas
    and J. P. Theobald, Nucl. Instr. and Methods 157 (1978) 301.

28) A. J. P. L. Policarpo, Nucl. Instr. and Methods 153 (1978) 389.

29) G. Charpak, A. Policarpo, and F. Sauli, IEEE NS 27, No. 1 (1980) 212.

30) J. Seguinot and T. Ypsilantis, Nucl. Instr. and Methods 142 (1977) 377.

31) G. Charpak, S. Majewski, G. Melchart, F. Sauli and T. Ypsilantis, Nucl. Instr. and Methods 164 (1979) 419.

32) M. H. Salamon and S. P. Ahlen, contribution to this conference.

33) J. B. Birks, The Theory and Practice of Scintillation Counting (Pergamon, Oxford, 1964).

34) S. P. Ahlen, Rev. Mod. Physics 52 (1980) 121.

35) F. D. Becchetti, C. E. Thorn and M. J. Levine, Nucl. Instr. and Methods 138 (1976) 93.

36) S. P. Ahlen, B. G. Cartwright and G. Tarlé, Nucl. Instr. and Methods 147 (1977) 321.

37) A. Meyer and R. B. Murray, Phys. Rev. 128 (1962) 98.

38) R. Voltz, J. Lopes da Silva, G. Laustriat and A. Coche, J. Chem. Phys. 45 (1966) 3306.

39) C. L. Ruiz, R. W. Huggett and P. N. Kirk, Nucl. Instr. and Methods 159 (1979) 55.

40) M. R. Maier, H. G. Ritter and H. H. Gutbrod, IEEE NS 27, No. 1 (1980) 42, and H. H. Gutbrod, M. R. Maier, J. Péter, A. M. Poskanzer, H. G. Ritter, H. Stelzer, R. Stock, A. I. Warwick, F. Weik and H. Wieman, contribution to this conference.

41) J. P. Alard et al., contribution to this conference.